Analytica Chimica Acta xxx (2017) 1–8

Contents lists available at ScienceDirect

Analytica Chimica Acta

journal homepage: www.elsevier.com/locate/aca

A novel dual-functional biosensor for fluorometric detection of inorganic pyrophosphate and pyrophosphatase activity based on globulin stabilized gold nanoclusters

Shenghao Xu [a], Xiuying Feng [a], Teng Gao [a], Ruizhi Wang [a, b], Yaning Mao [a], Jiehua Lin [a], Xijuan Yu [a], Xiliang Luo [a, *]

[a] Key Laboratory of Sensor Analysis of Tumor Marker Ministry of Education, College of Chemistry and Molecular Engineering, Qingdao University of Science and Technology, Qingdao 266042, PR China
[b] College of Polymer Science and Engineering, Qingdao University of Science and Technology, Qingdao 266042, PR China

HIGHLIGHTS

- A novel dual-functional biosensor for the detection of PPi and PPase is developed.
- The biosensor provides a low detection limit for PPi and PPase.
- The biosensor can be used for the assaying of PPase activity in human serum.
- Globulin protected gold nanoclusters with excellent stability are synthesized.

GRAPHICAL ABSTRACT

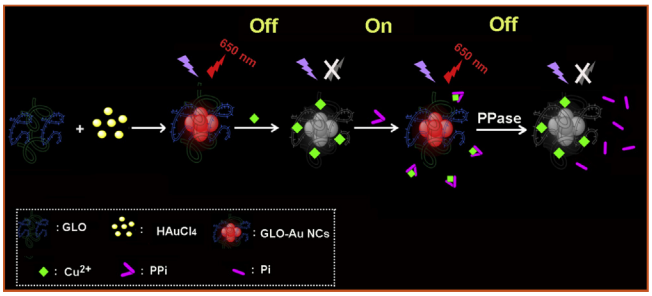

ARTICLE INFO

Article history:
Received 3 June 2016
Received in revised form
3 November 2016
Accepted 19 December 2016
Available online xxx

Keywords:
Dual-functional biosensor
Gold nanoclusters
Off on off
Competitive response
Fluorescence

ABSTRACT

A novel ultrasensitive dual-functional biosensor for highly sensitive detection of inorganic pyrophosphate (PPi) and pyrophosphatase (PPase) activity was developed based on the fluorescent variation of globulin protected gold nanoclusters (Glo@Au NCs) with the assistance of Cu^{2+}. Glo@Au NCs and PPi were used as the fluorescent indicator and substrate for PPase activity evaluation, respectively. In the presence of Cu^{2+}, the fluorescence of the Glo@Au NCs will be quenched owing to the formation of Cu^{2+}-Glo@Au NCs complex, while PPi can restore the fluorescence of the Cu^{2+}-Glo@Au NCs complex because of its higher binding affinity with Cu^{2+}. As PPase can catalyze the hydrolysis of PPi, it will lead to the release of Cu^{2+} and re-quench the fluorescence of the Glo@Au NCs. Based on this mechanism, quantitative evaluation of the PPi and PPase activity can be achieved ranging from 0.05 μM to 218.125 μM for PPi and from 0.1 to 8 mU for PPase, with detection limits of 0.02 μM and 0.04 mU, respectively, which is much lower than that of other PPi and PPase assay methods. More importantly, this ultrasensitive dual-functional biosensor can also be successfully applied to evaluate the PPase activity in human serum, showing great promise for practical diagnostic applications.

1. Introduction

Monitoring of enzyme activity has attracted great interest because of its potential application in diagnosis, prognosis, and

* Corresponding author.
E-mail address: xiliangluo@qust.edu.cn (X. Luo).

http://dx.doi.org/10.1016/j.aca.2016.12.026
0003-2670/

treatment of diseases. Inorganic pyrophosphatase (PPase), an elementary metal-dependent hydrolysis enzyme which could specifically catalyze the conversion of one molecule of inorganic pyrophosphate (PPi) into two orthophosphate (Pi) ions [1,2], plays central roles in many biological processes such as calcium absorption, lipid metabolism, bone formation and other biochemical transformations [3,4]. PPi, an abundant phosphate species in biological systems, is involved in many enzyme-catalyzed biosynthesis where it plays various important roles. Consequently, sensitive and fast detection of PPi and PPase activity are of sustained attention due to its urgent and important significance for investigating the PPi and PPase-related biological processes and disease diagnosis. Thus far, several techniques have been developed to detect PPi (fluorescent chemosensor and magnetic nanoparticle [5,6]) and PPase activity (chemiluminescent, enzymatic and colorimetric methods [7,8]). Nevertheless, these methods suffer from either time-consuming procedures, expensive cost or relatively low sensitivity, which limit their widespread application for routine detection [9]. Therefore, simple, convenient, economic and sensitive methods for sensitive PPi and PPase activity detection still remain a challenge.

As a promising and burgeoning category of fluorophores, biomolecule templated metal nanoclusters, especially protein protected gold nanoclusters (Au NCs), have attracted considerable attention because of the three-dimensional (3D) complexed structures which can withstand a wide range of pH and can be easily conjugated with other biosystems [10–14]. Up to now, various proteins have been developed for the preparation of fluorescent Au NCs including trypsin, bovine serum albumin, transferring, pepsin, insulin, lysozyme and horseradish peroxidase, etc [15–18]. Their convenient synthesis strategies, excellent biocompatibility and prominent stability, along with the sensitive fluorescence switching behaviour are beneficial for the development of Au NCs-based enzyme activity assays [19]. Nevertheless, there have been scarce previous studies reporting on protein directed synthesis of fluorescent Au NCs for assessing enzyme (such as PPase) activity [20–22]. In view of the importance of this research topic, the development of novel protein directed synthesis of fluorescent Au NCs with lower synthetic demands, which can be used for assessing PPase activity are still of great significance.

In this work, globulin protected gold nanoclusters (Glo@Au NCs) with prominent photo-stability (pH-, temperature-, salt- and time-stability) and excellent water dispersibility have been successfully synthesized and were systematically characterized by using high-resolution transmission electron microscopy (HRTEM), atomic force microscope (AFM), ultraviolet absorption spectroscopy, fluorescence spectroscopy, X-ray photoelectron spectroscopy (XPS), X-Ray Diffraction (XRD) and infrared (IR) spectroscopy. Subsequently, taking advantage of the good biocompatibility and strong fluorescence of the Glo@Au NCs, in combination with the unique fluorescence quenching of Glo@Au NCs caused by Cu^{2+}, effective fluorescence recovery induced by competitive interaction of PPi to Cu^{2+}, and hydrolysis ability of PPase to PPi, an ultrasensitive dual-functional biosensor capable of detecting PPi (turn on) and PPase activity (turn off) was established. As the synthetic strategy of the Glo@Au NCs is simple and convenient, and there is no tedious organic reaction involved during the whole experiment, this dual-functional biosensor offers an excellent and facile method for the evaluation of PPi and PPase activity. Furthermore, owing to the combination of enzymatic hydrolysis reaction with the off-on-off fluorescent sensing mechanism, this biosensor is highly selective and sensitive (with a detection limit of 0.04 mU), and can be successfully applied to the quantitative monitoring of PPase activity in human serum samples.

2. Materials and methods

2.1. Materials

All reagents were of analytical reagent grade. $HAuCl_4 \cdot 3H_2O$ (Hydrogen tetrachloroaurate trihydrate), pyrophosphatase (EC 3.6.1.1), inorganic from baker's yeast (Saccharomyces cerevisiae) and Y-Globulin were obtained from Sigma-Aldrich (USA). Copper (II) sulfate pentahydrate ($CuSO_4 \cdot 5H_2O$), pyrophosphate (PPi) and sodium hydroxide (NaOH) and other salts were purchased from Aladdin Ltd. Water was obtained through a Millipore Milli-Q water system. Serum sample were obtained from the Affiliated Hospital of the Beijing Normal University, and the sample was collected with informed consent from the human subject. In addition, this sample collection was approved by Institutional Review Board of Beijing Ditan Hospital.

2.2. Instruments

The morphology and size of Glo@AuNCs were characterized by a JEM-2100 transmission electron microscope (TEM) with an accelerating voltage of 200 kV. Fluorescence spectra were recorded by an F-4600 fluorescence spectrometer. Height characterization was performed by atomic force microscopy (AFM) (from Veeco with a IIIa controller) operating in tapping mode. X-ray diffraction (XRD) patterns in the Bragg' s angle (2θ) range of 20–80° were collected at room temperature by using a Bruker D8 diffractometer with Cu Kα radiation. X-ray photoelectron spectroscopy (XPS) was performed on a thermoelectron instrument (Thermo-VG Sci-entific ESCALAB 250), and all spectra were referenced to the C 1s peak at 285.0 eV. Infrared spectra (IR) were recorded using a FT/IR-410 Fourier transform infrared spectrophotometer (JASCO, Japan). UV–vis absorption spectra were recorded by a CARY 500 UV–vis–NIR Varian spectrophotometer using a 1 cm path length quartz cell at room temperature.

2.3. Preparation of Glo@Au NCs

All glassware were washed with aqua regia and rinsed with ultrapure water. Typically, Y-Globulin (0.25 g) was dissolved in water (5.0 mL), then 5.0 mL of 10.0 mM $HAuCl_4$ was added under vigorous stirring, and the color of this solution turns from colorless to light-yellow. After 2 min, NaOH solution (1.0 mL, 1.0 M) was introduced, and the mixture was incubated at 37 °C for 6 h. The color of the solution changed from light-yellow to deep brown. The prepared Glu@Au NCs solution was stored at 4 °C before use.

2.4. Fluorescent PPase activity assay

The prepared NCs solution was diluted 100 times using phosphate buffer solution (PBS, pH 7.4) and marked as Glo@Au NCs (1/100), for the real-time PPase assays. 5 μL of PPase with different activities ranging from 0 to 10 mU was respectively added to 200 μL of the aforementioned Au NCs solution (1/100) containing Cu^{2+} (18.75 μM), PPi (218.125 μM) and Mg^{2+} (0.1 μM). After a brief mixing (1 min), the fluorescence spectra of the mixture were recorded respectively.

3. Results and discussion

3.1. Synthesis and characterization of Glo@Au NCs

Fig. 1A presents a typical transmission electron microscopy (TEM) image of the prepared Glo@Au NCs, revealing that they are spherical with good monodispersity. Moreover, the well-resolved

Please cite this article in press as: S. Xu, et al., A novel dual-functional biosensor for fluorometric detection of inorganic pyrophosphate and pyrophosphatase activity based on globulin stabilized gold nanoclusters, Analytica Chimica Acta (2017), http://dx.doi.org/10.1016/j.aca.2016.12.026

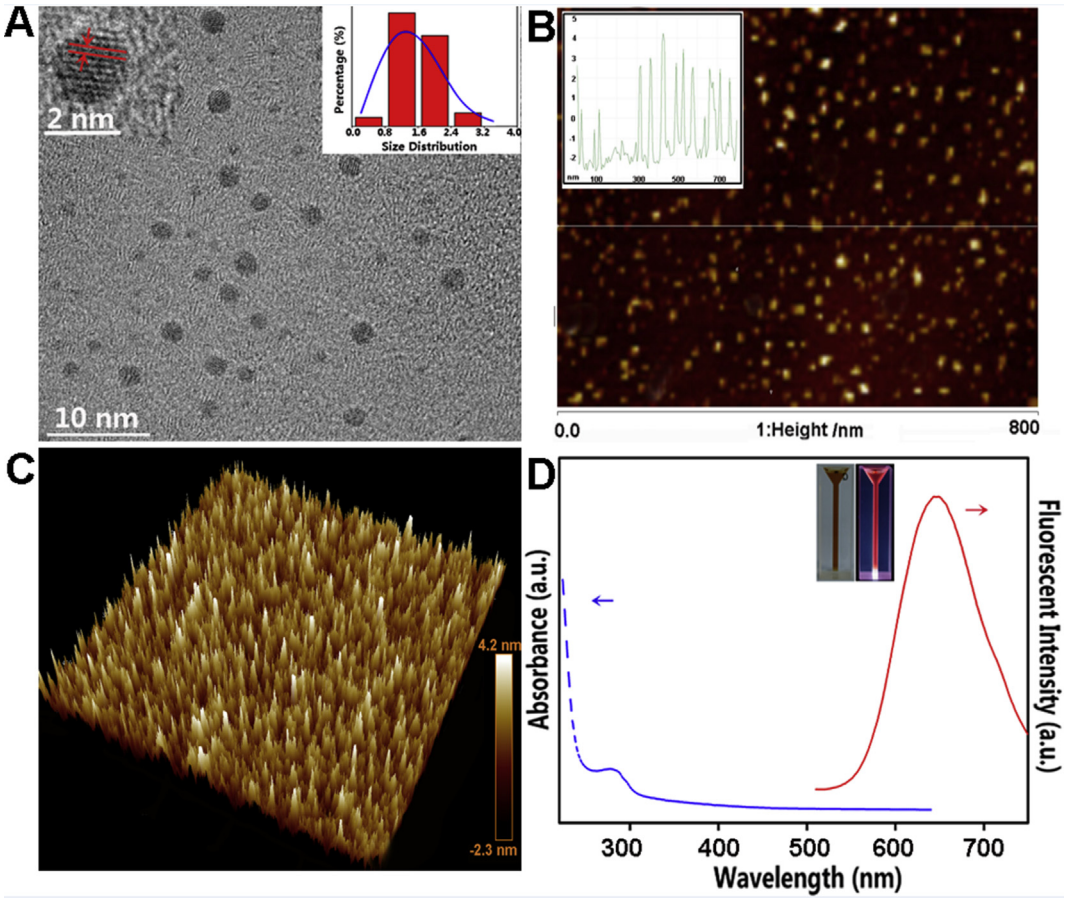

Fig. 1. (A) Typical TEM image of the Glo@Au NCs, inset displays the HRTEM image and size distribution histogram of the Glo@Au NCs. (B) AFM image (2D) of the Glo@Au NCs (C) AFM image (3D) of the Glo@Au NCs. (D) Absorption spectra (blue line) and emission (red line) spectra of the Glo@Au NCs, inset shows photographs of the Au NCs under sunlight (left) and 365 nm UV light illumination (right). (For interpretation of the references to colour in this figure legend, the reader is referred to the web version of this article.)

lattice planes with a spacing of ~0.23 nm (corresponding to the d-spacing of the {111} crystal plane of Au) in the HRTEM image (inset in Fig. 1A) shows the prominent crystalline structure of the Glo@Au NCs, which is in accordance with the previous report [23]. The diameter histogram in the inset in Fig. 1A, calculated by measuring more than 100 particles in the TEM image, shows that the Glo@Au NCs have an average size of about 1.76 nm. Fig. 1B and C shows the typical two-dimensional and three-dimensional AFM image of the monodispersed Au NCs on freshly cleaned mica surfaces, the topographic morphology with small spherical dots and cross-sectional heights of the Au NCs were consistent with our TEM data. The prepared Glo@Au NCs shows a broad absorption band in the UV region and the absence of plasmon resonance bands of larger Au nanoparticles in the visible region, suggesting the successful formation of Au NCs (Fig. 1D). Additionally, the fluorescence emission was also investigated to confirm the formation of Glo@Au NCs. As shown in Fig. 1D, the prepared Glo@Au NCs, with a quantum yield (QY) of 5.6% (calibrated with rhodamine B as the reference), exhibit strong red fluorescence with an emission maximum at 650 nm.

In order to obtain additional information about the Glo@Au NCs, XPS was carried out and the results are shown in Fig. 2A. The binding energy of the Au $4f_{5/2}$ and Au $4f_{7/2}$ peaks are 84.13 and 87.83 eV, respectively, indicating that both Au^0 and Au^+ exist in the Glo@Au NCs [24]. Moreover, the Au(I) surrounded on the surface of gold core is beneficial for the stabilization of the Au NCs [25], and it is proved that the Glo@Au NCs are relatively stable and the fluorescence quenching only occurred slightly after two months of storage in darkness at 4 °C (Fig S1A, see Supporting Information). In addition, they also have high stability under various pH values, different concentrations of NaCl and various temperatures (Fig S1B to D, see Supporting Information). Moreover, the S 2p3/2 peak at 163.1 eV (Fig. 2B) corresponding to a gold thiolate again confirms the covalent interaction of AuNCs with the sulfhydryl group of Glo [26]. It is noteworthy that the typical peak representing oxidized sulfur (at about 168 eV) is absent from the S(2p) region in Glo@AuNCs, suggesting that this approach used here was gentler for preparing Glo@AuNCs [27].

Consistent results were obtained in XRD measurements. The structures of the Glo@Au NCs were then examined by XRD measurements. As shown in Fig. 2C, four additional diffraction peaks emerged at $2\theta = 38.1°$, 44.2°, 64.7°, and 77.8°, which are in keeping with the (111), (200), (220) and (311) diffractions of fcc gold (JCPDS 75-2870) [28]. Comparison of the IR spectra of globulin and Glo@Au NCs demonstrates that the functionalization of Glo to AuNCs led to a shift of the peak corresponding to the amide in Glo at wave numbers from 1656 to 1664 cm^{-1} (Fig. 2D). Such shift is possibly related to a modification of the structure of the protein backbone primarily because of the interaction of Glo and Au. Additionally, the IR spectra of Glo@AuNCs shows the characteristic bands for primary amines at 1531 cm^{-1} and 3306 cm^{-1}, C-H vibration band at 2958 cm^{-1}, indicating the presence of Glo in the prepared Glo@Au NCs (Fig. 2D). Furthermore, a systematic study was performed to investigate the optimal conditions (e.g. the concentration of $HAuCl_4$, NaOH and globulin, respectively) for preparing the highly fluorescent Glo@Au NCs. As shown in Fig S2, an optimal

Please cite this article in press as: S. Xu, et al., A novel dual-functional biosensor for fluorometric detection of inorganic pyrophosphate and pyrophosphatase activity based on globulin stabilized gold nanoclusters, Analytica Chimica Acta (2017), http://dx.doi.org/10.1016/j.aca.2016.12.026

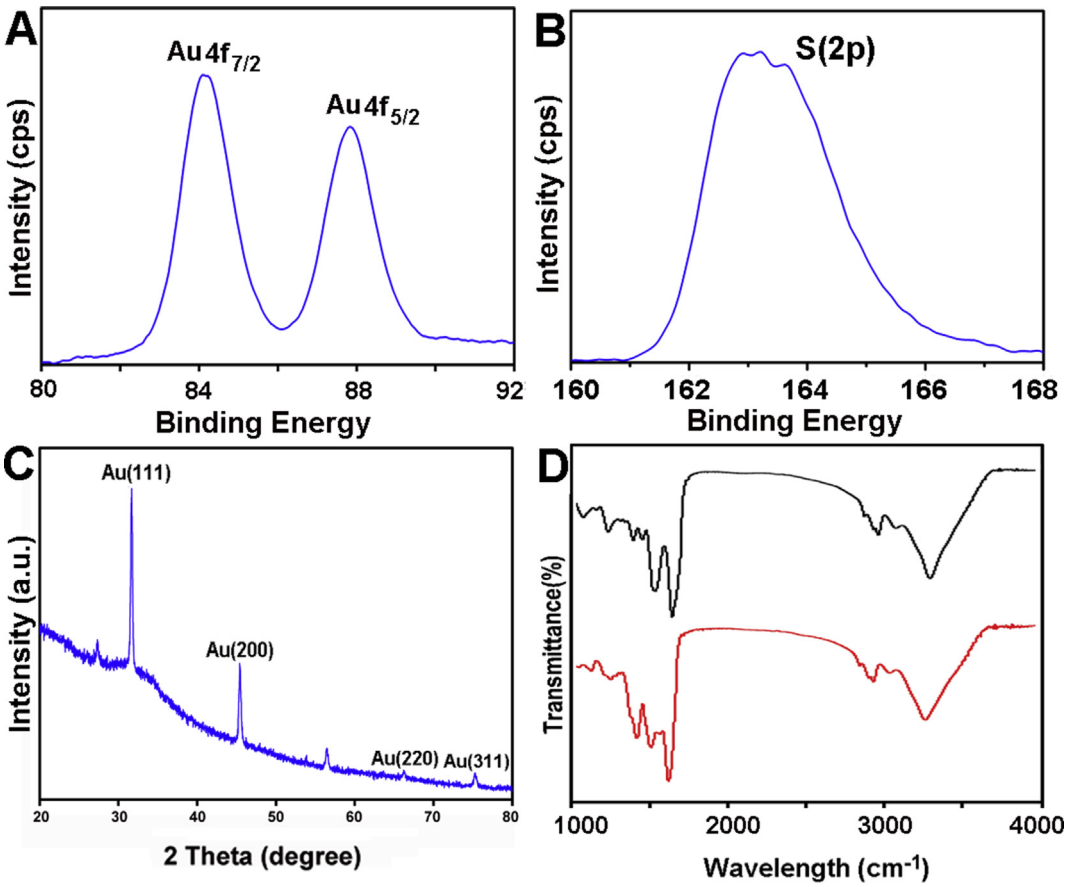

Fig. 2. (A) Au 4f electron region of the XPS of the Glo@Au NCs. (B) S 2p electron region of the XPS of the Glo@Au NCs. (C) XRD patterns of the Glo@Au NCs. (D) Infrared spectroscopy of the globulin and the as-prepared Glo@Au NCs.

composition of 10 mM $HAuCl_4$, 1.0 M NaOH and 50 mg/mL of globulin generates the highest red emission of the Glo@Au NCs.

3.2. Principle of the dual-functional biosensor

A highly sensitive dual-functional biosensor for PPi and PPase activity detection was developed inspired by the competitive binding of Cu^{2+} between fluorescent Glo@Au NCs and PPi, accompanied by a fluorescence turn off-on-off process (Scheme 1). As shown in Fig. 3, the red fluorescence of the Glo@Au NCs (1/100) could be immediately quenched in the presence of Cu^{2+} (18.75 μM), which may be resulted from the coordination of Cu^{2+} with the

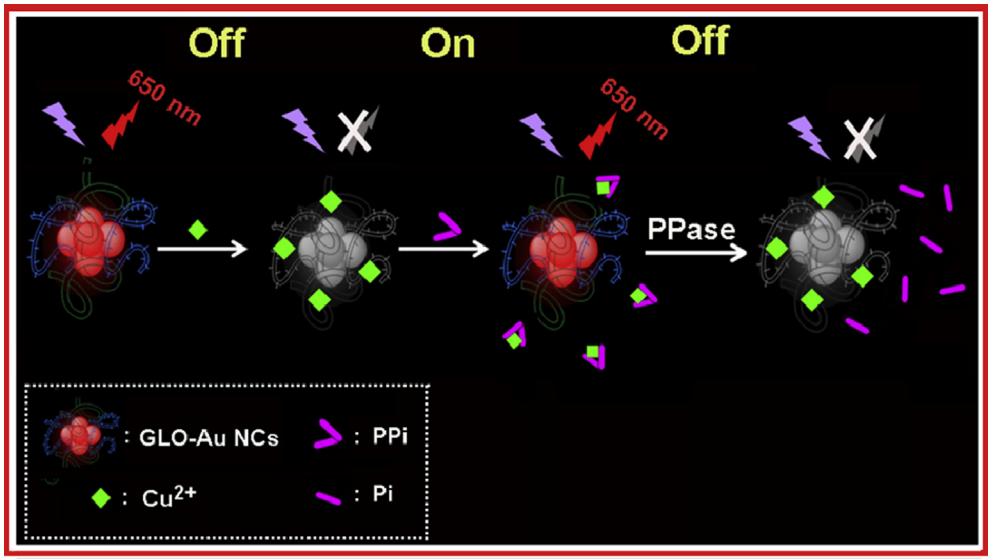

Scheme 1. Schematic representation of the ultrasensitive biosensor based on the competitive binding of Cu^{2+} between Glo@Au NCs and PPi.

Please cite this article in press as: S. Xu, et al., A novel dual-functional biosensor for fluorometric detection of inorganic pyrophosphate and pyrophosphatase activity based on globulin stabilized gold nanoclusters, Analytica Chimica Acta (2017), http://dx.doi.org/10.1016/j.aca.2016.12.026

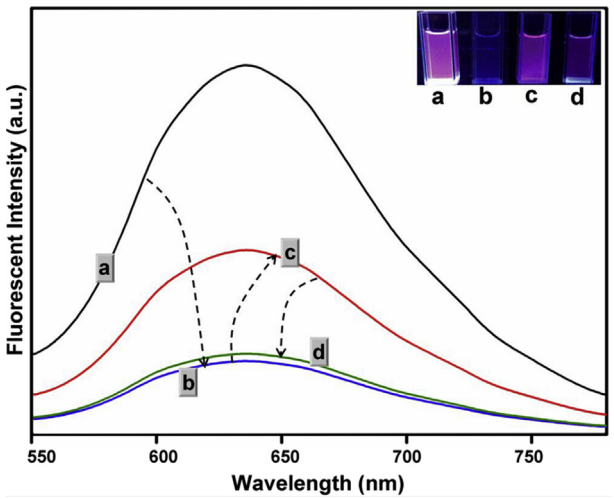

Fig. 3. Fluorescence emission spectra and photographs (inset) under UV light of the Glo@Au NCs (a), Glo@Au NCs + Cu^{2+} (b), Glo@Au NCs + Cu^{2+} + PPi (c), and Glo@Au NCs + Cu^{2+} + PPi + PPase (d) in PBS (pH 7.4).

carboxyl group of globulin, and the formation of Glo@Au NCs-Cu^{2+} complexes. Thus, effective charge transfer from Glo@Au NCs to Cu^{2+} was built and the Au-S charge transfer in the interface of the Glo@Au NCs would be blocked [29,30]. Nevertheless, the fluorescence could be partially recovered within seconds by the addition of PPi (218.125 μM), as PPi would preferentially bind to Cu^{2+} with higher affinity, and effectively recapture the Cu^{2+} from the surface of the Glo@Au NCs [31,32]. Therefore, the quantitative detection of PPi could be realized based on the fluorescence signal recovery. Finally, PPase was introduced into the solution containing Glo@Au NCs-Cu^{2+}-PPi to catalyze the hydrolysis of PPi to Pi (which is unable to complex with Cu^{2+}), allowing the release of Cu^{2+}. Therefore, the free Cu^{2+} will bind to Glo@Au NCs and cause the fluorescence quenched again. Based on this mechanism, a real-time ultrasensitive dual-functional biosensor for PPi and PPase activity detection was established.

3.3. PPi and PPase activity detection based on the dual-functional biosensor

Firstly, conditions for PPase assay, including the added amount of Cu^{2+} and PPi were optimized. As shown in Fig. 4A and B, the fluorescence of the Glo@Au NCs (1/100) was gradually quenched with the increasing concentration of Cu^{2+} (0–37.5 μM). In the presence of 18.75 μM Cu^{2+}, approximately 90% of the initial fluorescence intensity of the Glo@Au NCs (1/100) was quenched, and this Cu^{2+} concentration was then adopted in the following experiments. Subsequently, the fluorescence intensity of the system could be gradually restored after the addition of different concentrations of PPi (Fig. 4C). An excellent linear correlation ($R^2 = 0.9942$) exists based on the fluorescent recovery effects (I/I_0) on the quencher concentration of PPi over the range from 0.05 to

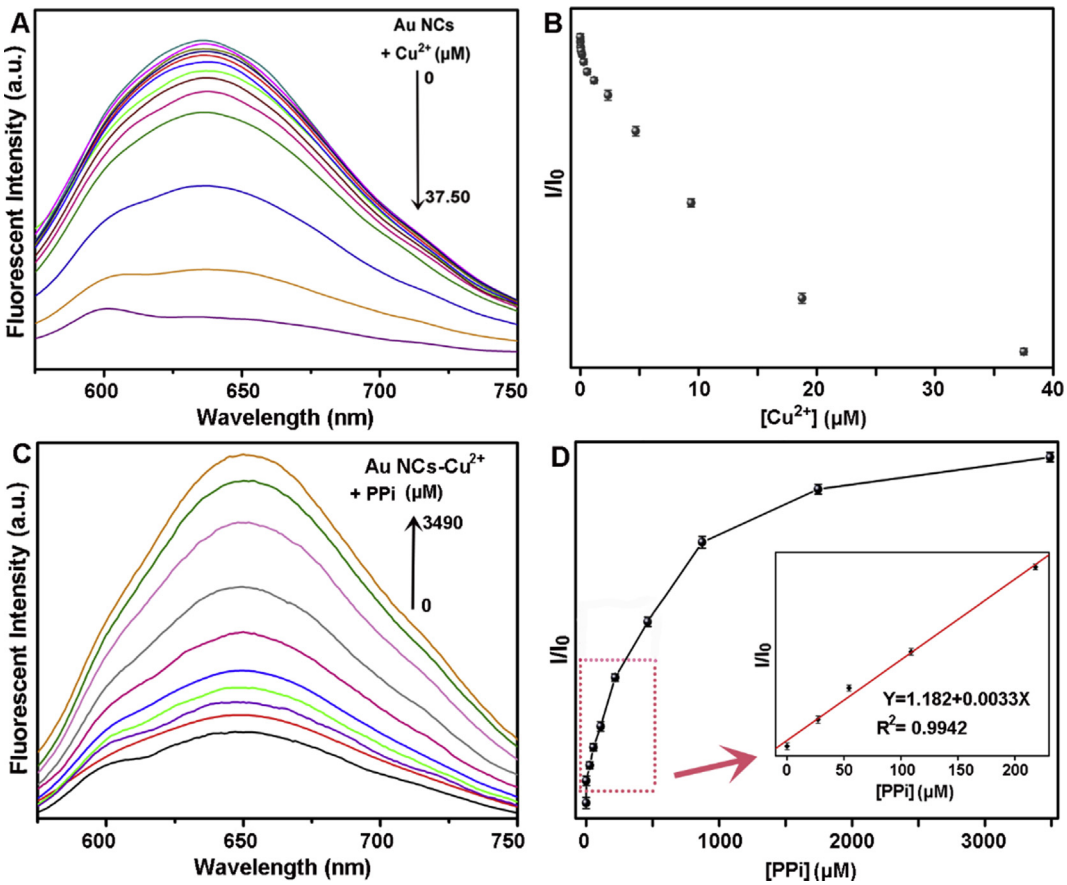

Fig. 4. (A) Fluorescence emission spectra of the Glo@Au NCs with the addition of different Cu^{2+} concentrations increasing from 0 to 37.5 μM. (B) Relative fluorescence intensity (I/I_0 at 650 nm) for Glo@Au NCs versus the Cu^{2+} concentrations. (C) Fluorescence emission spectra of the Glo@Au NCs-Cu^{2+} complexes with addition of different PPi concentrations increasing from 0 to 3490 μM. (D) Relative fluorescence intensity (I/I_0 at 650 nm) for Glo@Au NCs -Cu^{2+} versus the PPi concentrations. Inset: expanded linear region. Measurements were carried out by using Glo@Au NCs (1/100) in 10 mM PBS (pH 7.4).

Please cite this article in press as: S. Xu, et al., A novel dual-functional biosensor for fluorometric detection of inorganic pyrophosphate and pyrophosphatase activity based on globulin stabilized gold nanoclusters, Analytica Chimica Acta (2017), http://dx.doi.org/10.1016/j.aca.2016.12.026

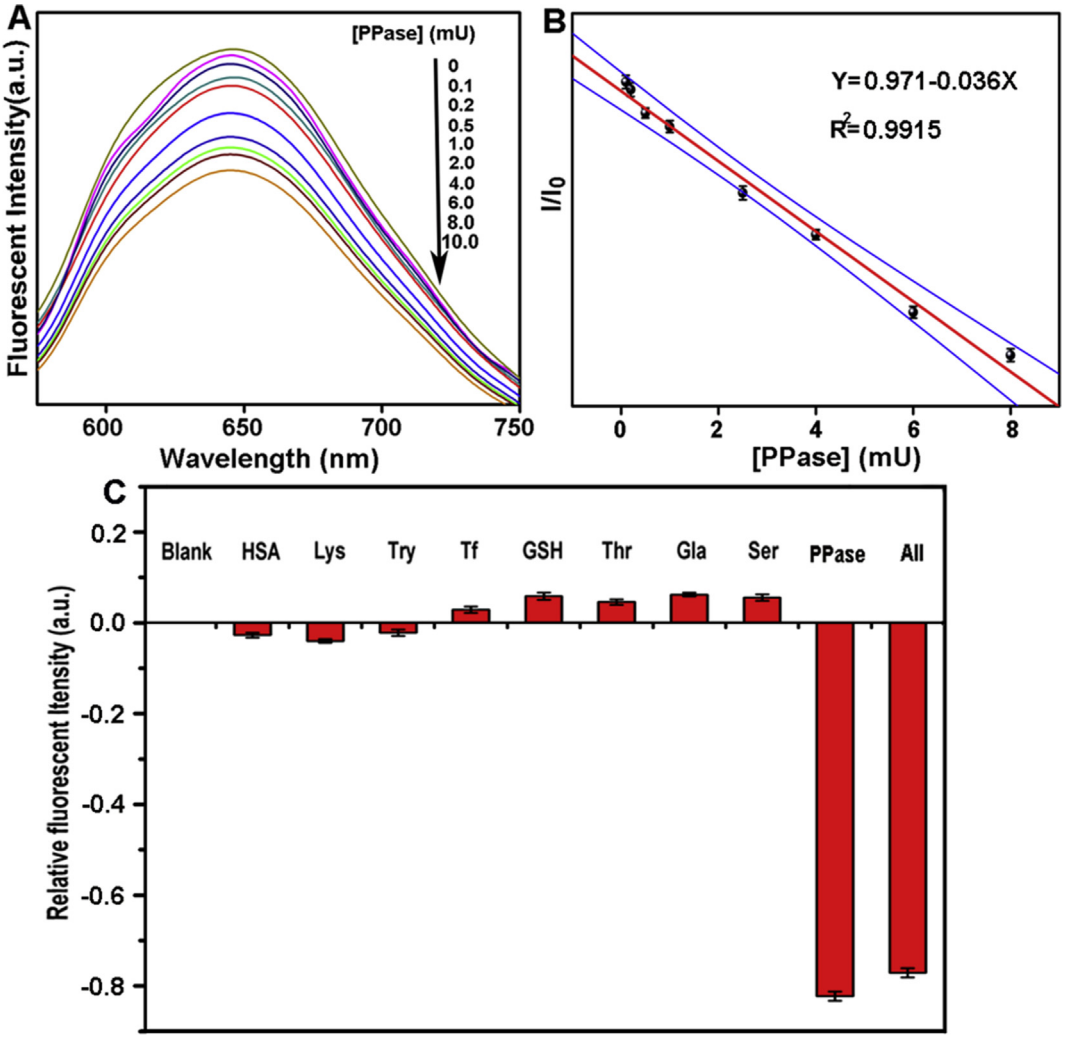

Fig. 5. (A) Changes in the emission spectrum of Glo@Au NCs (1/100) containing Cu^{2+} (18.75 μM), PPi (218.125 μM) and Mg^{2+} (0.1 μM) after adding PPase in different concentrations. (B) Plot of the relative fluorescence intensity versus the PPase concentrations. (C) Relative fluorescence intensity (I/I_0 at 650 nm) of Glo@Au NCs (1/100) containing Cu^{2+} (18.75 μM), PPi (218.125 μM) and Mg^{2+} (0.1 μM) after adding the control biomolecules only (2.0 μg/mL proteins or 1 μM GSH), and coexistence of 10 mU PPase (red columns) at room temperature. (For interpretation of the references to colour in this figure legend, the reader is referred to the web version of this article.)

218.125 μM. The detection limit is found to 0.02 μM (Fig. 4D) using 3σ/S method (where s is the standard deviation of the blank signal and S is the slope of the linear calibration plot [33]), which is lower than the recent reports [34,35]. And this linear relationship between the fluorescence intensity ratios of the Glo@Au NCs (1/100) and the concentrations of PPi would be beneficial to the subsequent real-time and quantitative PPase activity assay. Hence, 218.125 μM PPi was chosen as the optimum concentration for PPase activity assay.

The activity of PPase was monitored using Glo@Au NCs (1/100) in 10 mM PBS (pH 7.4) containing Cu^{2+} (18.75 μM), PPi (218.125 μM) and Mg^{2+} (0.1 μM) as the standard assay solution. Related reactions were recorded by fluorescence emission spectroscopy after adding different activity units of PPase at room temperature. As shown in Fig. 5A, the emission intensity at 650 nm is gradually reduced with increasing the PPase concentration. A linear correlation was obtained based on the quenching effects (I/I_0) on the quencher concentration of PPase over the range from 0.1 to 8 mU. The detection limit is found to 0.04 mU (Fig. 5B) using 3σ/S method (where s is the standard deviation of the blank signal and S is the slope of the linear calibration plot [32]), which is significantly lower than that of most previously reported methods [7,36].

In addition to good sensitivity, highly special response to the analyte over potentially competing species is also a requirement for an assay in biomedical and environmental systems. Therefore, the selectivity of the dual-functional biosensor to PPase over other

Table 1
Detection results of PPase in human serum.

Sample	Spiked amount (mU)	Detected amount (mU)	Recovery (%)	RSD (%), n = 5
1	0	0.02	–	–
2	2.0	2.03 ± 0.05	101.50	2.46
3	4.0	4.14 ± 0.04	103.50	0.97
4	8.0	7.86 ± 0.12	98.25	1.53

Please cite this article in press as: S. Xu, et al., A novel dual-functional biosensor for fluorometric detection of inorganic pyrophosphate and pyrophosphatase activity based on globulin stabilized gold nanoclusters, Analytica Chimica Acta (2017), http://dx.doi.org/10.1016/j.aca.2016.12.026

potential coexistent biocomponents such as 2.0 μg/mL of HSA, Lys, Try, Tf and 1 μM of GSH, Thr, Gla and Ser were investigated in control experiments. As shown in Fig. 5C, these potentially coexisted biological components had minor or negligible quenching effects on the fluorescence intensity, even the added concentration of the control proteins (2.0 μg/mL) is much higher than the amount of PPase in the assay. These results revealed that this dual-functional biosensor had high sensitivity and excellent selectivity toward PPase.

3.4. Detection of PPase in human serum

To further explore the potential practical application of this ultrasensitive dual-functional biosensor, the recovery rates of different concentrations of PPase in human serum were detected. We selected three final PPase concentrations (2, 4, and 8 mU), which are in the liner range from 0.1 to 8 mU for the real sample test. As shown in Table 1 in the supporting information, the recoveries were acceptable, ranging from 98.25 to 103.50%, indicating great potential of this bioassay for quantitative determination of PPase in human serum samples.

4. Conclusions

In summary, Glo@Au NCs with unique optical properties have been synthesized and characterized in detail. With the assistance of competitive coordination between Cu^{2+} and PPi, we have established a simple and novel fluorescent bioassay for PPase activity detection with a super high sensitivity and ultralow detection limit (0.04 mU), which is superior to previous reports. Moreover, combining the enzymatic hydrolysis reaction with the off-on-off fluorescent sensing mechanism, the dual-functional biosensor is highly selective and can be successfully applied to the quantitative determination of PPase in human serum samples. It is expected that the present work may not only offer a general route for the synthesis of protein templated fluorescent Au NCs, but also accelerate the development of competitive fluorescent biosensors.

Acknowledgements

The authors gratefully acknowledge the support from the National Nature Science Foundation of China (21275087, 21422504, 21505081), the Natural Science Foundation of Shandong Province of China (JQ201406, ZR2013BQ004), the Taishan Scholar Program of Shandong Province, and the Science and Technology Project of Shandong Province (J15LC14).

Appendix A. Supplementary data

Supplementary data related to this article can be found at http://dx.doi.org/10.1016/j.aca.2016.12.026.

References

[1] E. Oksanen, A.K. Ahonen, H. Tuominen, V. Tuominen, R. Lahti, A. Goldman, P. Heikinheimo, A complete structural description of the catalytic cycle of yeast pyrophosphatase, Biochemistry 46 (2007) 1228–1239.
[2] D.H. Vance, A.W. Czarnik, Real-time assay of inorganic pyrophosphatase using a high-affinity chelation-enhanced fluorescence chemosensor, J. Am. Chem. Soc. 116 (1994) 9397–9398.
[3] C. Guarise, L. Pasquato, V.D. Filippis, P. Scrimin, Gold nanoparticles-based protease assay, Proc. Natl. Acad. Sci. U.S.A. 103 (2006) 3978–3982.
[4] G.M. Carman, G.S. Han, Roles of phosphatidate phosphatase enzymes in lipid metabolism, Trends Biochem. Sci. 31 (2006) 694–699.
[5] A. Gogoi, S. Mukherjee, A. Ramesh, G. Das, Aggregation-induced emission active metal-free chemosensing platform for highly selective turn-on sensing and bioimaging of pyrophosphate anion, Anal. Chem. 87 (2015) 6974–6979.
[6] L.L. Tong, Z.Z. Chen, Z.Y. Jiang, M.M. Sun, L. Li, J. Liu, B. Tang, Fluorescent sensing of pyrophosphate anion in synovial fluid based on DNA-attached magnetic nanoparticles, Biosens. Bioelectron. 72 (2015) 51–55.
[7] J.J. Deng, Q. Jiang, Y.X. Wang, L.F. Yang, P. Yu, L.Q. Mao, Real-time colorimetric assay of inorganic pyrophosphatase activity based on reversibly competitive coordination of Cu2+ between cysteine and pyrophosphate ion, Anal. Chem. 85 (2013) 9409–9415.
[8] Q. Zhou, Y.X. Lin, M.D. Xu, Z.Q. Gao, H.H. Yang, D.P. Tang, Facile synthesis of enhanced fluorescent gold–silver bimetallic nanocluster and its application for highly sensitive detection of inorganic pyrophosphatase activity, Anal. Chem. 88 (2016) 8886–8892.
[9] N. Malashikhina, G.G. Ibabe, V. Pavlov, Unconventional application of conventional enzymatic substrate: first fluorogenic immunoassay based on enzymatic formation of quantum dots, Anal. Chem. 85 (2013) 6866–6870.
[10] K. Kwak, S.S. Kumar, K. Pyo, D. Lee, Ionic liquid of a gold nanocluster: a versatile matrix for electrochemical biosensors, ACS Nano 8 (2014) 671–679.
[11] S.H. Xu, P.P. Liu, Q.W. Song, L. Wang, X.L. Luo, One-pot synthesis of biofunctional and near-infrared fluorescent gold nanodots and their application in Pb2+ sensing and tumor cell imaging, RSC Adv. 5 (2015) 3152–3156.
[12] X.M. Yang, Y.W. Luo, Y. Zhuo, Y.J. Feng, S.S. Zhu, Novel synthesis of gold nanoclusters templated with L-tyrosine for selective analyzing tyrosinase, Anal. Chim. Acta 840 (2014) 87–92.
[13] S.H. Xu, X.L. Li, Y.N. Mao, T. Gao, X.Y. Feng, X.L. Luo, Novel dual ligand cofunctionalized fluorescent gold nanoclusters as a versatile probe for sensitive analysis of Hg2+ and oxytetracycline, Anal. Bioanal. Chem. 408 (2016) 2955–2962.
[14] S.H. Xu, T. Gao, X.Y. Feng, Y.N. Mao, P.P. Liu, X.J. Yu, X.L. Luo, Dual ligand cofunctionalized fluorescent gold nanoclusters for the “turn on” sensing of glutathione in tumor cells, J. Mater. Chem. B 4 (2016) 1270–1275.
[15] T. Chen, W. Tseng, (Lysozyme type VI)-stabilized Au8 clusters: synthesis mechanism and application for sensing of glutathione in a single drop of blood, Small 8 (2012) 1912–1919.
[16] H. Kawasaki, K. Hamaguchi, I. Osaka, R. Arakawa, ph-Dependent synthesis of pepsin-mediated gold nanoclusters with blue green and red fluorescent emission, Adv. Funct. Mater. 21 (2011) 3508–3515.
[17] C. Liu, H. Wu, Y. Hsiao, C. Lai, C. Shih, Y. Peng, K. Tang, H. Chang, Y. Chien, J. Hsiao, J. Cheng, P. Chou, Insulin-directed synthesis of fluorescent gold nanoclusters: preservation of insulin bioactivity and versatility in cell imaging, Angew. Chem. Int. Ed. 50 (2011) 7056–7060.
[18] S.H. Xu, X. Lu, C.X. Yao, F. Huang, H. Jiang, W.H. Hua, N. Na, H.Y. Liu, J. Ouyang, A visual sensor array for pattern recognition analysis of proteins using novel blue-emitting fluorescent gold nanoclusters, Anal. Chem. 86 (2014) 11634–11639.
[19] Y. Chen, H.P. Zhou, Y. Wang, W.Y. Li, J. Chen, Q. Lin, C. Yu, Substrate hydrolysis triggered formation of fluorescent gold nanoclusters–a new platform for the sensing of enzyme activity, Chem. Commun. 49 (2013) 9821–9823.
[20] J. Sun, F. Yang, D. Zhao, X.R. Yang, Highly sensitive real-time assay of inorganic pyrophosphatase activity based on the fluorescent gold nanoclusters, Anal. Chem. 86 (2014) 7883–7889.
[21] H.H. Deng, F.F. Wang, X.Q. Shi, H.P. Peng, A.L. Liu, X.H. Xia, W. Chen, Water-soluble gold nanoclusters prepared by protein-ligand interaction as fluorescent probe for real-time assay of pyrophosphatase activity, Biosens. Bioelectron. 83 (2016) 1–8.
[22] X.L. Zhu, J.W. Liu, H.Y. Peng, J.H. Jiang, R.Q. Yu, A novel fluorescence assay for inorganic pyrophosphatase based on modulated aggregation of graphene quantum dots, Analyst 141 (2016) 251–255.
[23] C. Zhou, C. Sun, M. Yu, Y. Qin, J. Wang, M. Kim, J. Zheng, Luminescent gold nanoparticles with mixed valence states generated from dissociation of polymeric Au (I) thiolates, J. Phys. Chem. C 114 (2010) 7727–7732.
[24] L. Shang, N. Azadfar, F. Stockmar, W. Send, V. Trouillet, M. Bruns, D. Gerthsen, G.U. Nienhaus, One-pot synthesis of near-infrared fluorescent gold clusters for cellular fluorescence lifetime imaging, Small 7 (2011) 2614–2620.
[25] A. Santosh, B.K.C. Remant, N. Dharmaraj, N. Bhattarai, C.H. Kim, H.Y. Kim, Spectroscopic identification of S Au interaction in cysteine capped gold nanoparticles, Spectrochim. Acta Part A 63 (2006) 160–163.
[26] G.A. Simms, J.D. Padmos, P. Zhang, Structural and electronic properties of protein/thiolate-protected gold nanocluster with “staple” motif: a XAS, L-DOS, and XPS study, J. Chem. Phys. 131 (2009) 214703.
[27] L. Guével, B. Hötzer, G. Jung, K. Hollemeyer, V. Trouillet, M. Schneider, Formation of fluorescent metal (Au, Ag) nanoclusters capped in bovine serum albumin followed by fluorescence and spectroscopy, J. Phys. Chem. C 115 (2011) 10955–10963.
[28] H. Qian, R. Jin, Controlling nanoparticles with atomic precision: the case of Au144 (SCH2CH2Ph) 60, Nano Lett. 9 (2009) 4083–4087.
[29] S.N. Yaliraki, M. Kemp, M.A. Ratner, Conductance of molecular wires: influence of molecule–electrode binding, J. Am. Chem. Soc. 121 (1999) 3428–3434.
[30] S. Roy, G. Palui, A. Banerjee, The as-prepared gold cluster-based fluorescent sensor for the selective detection of as III ions in aqueous solution, Nanoscale 4 (2012) 2734–2740.
[31] J.J. Deng, P. Yu, L.F. Yang, L.Q. Mao, Competitive coordination of Cu^{2+} between cysteine and pyrophosphate ion: toward sensitive and selective sensing of pyrophosphate ion in synovial fluid of arthritis patients, Anal. Chem. 85 (2013) 2516–2522.
[32] H. Yoon, J.M. Lim, H. Gee, C. Lee, Y. Jeong, D. Kim, W. Jang, A porphyrin-based

molecular tweezer: guest-induced switching of forward and backward photoinduced energy transfer, J. Am. Chem. Soc. 136 (2014) 1672–1679.
[33] Z.Q. Cheng, Z.Y. Wang, D.E. Gillespie, C. Lausted, Z. Zheng, M. Yang, J.S. Zhu, Plain silver surface plasmon resonance for microarray application, Anal. Chem. 87 (2015) 1466–1469.
[34] L. Wang, Q.W. Song, Q.L. Liu, D.C. He, J. Ouyang, Plasmon-Enhanced fluorescence-based core–shell gold nanorods as a near-IR fluorescent turn-on sensor for the highly sensitive detection of pyrophosphate in aqueous solution, Adv. Funct. Mater. 25 (2015) 7017–7027.
[35] Z.J. Hai, Y.J. Bao, Q.Q. Miao, X.Y. Yi, G.L. Liang, Pyridine–biquinoline–metal complexes for sensing pyrophosphate and hydrogen sulfide in aqueous buffer and in cells, Anal. Chem. 87 (2015) 2678–2684.
[36] S. Yang, G. Feng, N.H. Williams, Highly selective colorimetric sensing pyrophosphate in water by a NBD-phenoxo-bridged dinuclear Zn (ii) complex, Org. Biomol. Chem. 10 (2012) 5606–5612.

Please cite this article in press as: S. Xu, et al., A novel dual-functional biosensor for fluorometric detection of inorganic pyrophosphate and pyrophosphatase activity based on globulin stabilized gold nanoclusters, Analytica Chimica Acta (2017), http://dx.doi.org/10.1016/j.aca.2016.12.026